ICLASS 2009, 11th Triennial International Annual Conference on Liquid Atomization and Spray Systems, Vail, Colorado USA, July 2009

Validation of the Eulerian Mesoscopic Approach in Particle-Charged Homogeneous Isotropic Decaying Turbulence in the scope of Large Eddy Simulation of Fuel Sprays

A. Vié[*,1], L. Martinez[1], S. Jay[1], A. Benkenida[1] and B. Cuenot[2]
[1]IFP, 1&4 av. de Bois-Préau, 92852 Rueil-Malmaison Cedex - FRANCE
[2]CERFACS, 42 av. G. Coriolis, 31057 Toulouse Cedex 1 - FRANCE

Abstract

This work is devoted to the simulation of Diesel like sprays using an Eulerian-Eulerian approach. For this purpose, the AVBP code is used to perform the computations. It solves the compressible Navier Stokes equations for reactive two phase flows with low dissipation schemes adapted to Large Eddy Simulation (LES). To simulate the liquid phase, the Mesoscopic Eulerian Formalism (MEF) developed by Fevrier et al. is used. In this approach, an analogy is made between particles of a dispersed liquid phase, and molecules in a gas. Starting from the Boltzmann equation, it allows to determine eulerian conservation equations. This formalism was first designed for dilute sprays. In order to simulate fuel sprays in engines, these models have been adapted to dense sprays by the addition of collision effects.

The formalism is validated by Direct Numerical Simulation (DNS) of homogeneous isotropic decaying turbulence, loaded with inertial particles. The carrier phase is initiated with a Passot-Pouquet spectrum. The particles are injected uniformly at the same velocity as the carrier phase.

For non-collisional simulations, results are compared to Eulerian/Lagrangian Discrete Particles Simulation (DPS), considered as a reference. Simulations are performed with one-way coupling drag force (no modification of the gas phase by the liquid phase). As the Stokes number is 1.2, strong preferential concentration effects are expected. Results show that the total energy decrease is well reproduced for both phases with the MEF approach, and that preferential concentration effects are in good agreement with DPS computations.

For collisional simulations, the results are analysed qualitatively. To allow a parametric study, the collision and relaxation time scales of the liquid phase are varied: the Stokes number is varied between 0.6 and 2.4 and the mean liquid volume fraction between 0.027% and 2.7%. Results show that all expected asymptotic behaviours are well exhibited.

Introduction

To simulate fuel sprays, two approaches are commonly used: Lagrangian and Eulerian methods. Lagrangian methods consist in tracking and moving each particles or parcels (group of particles). But for industrial applications, the number of particles required to obtain correct statistics is high and demands multiprocessor computations with efficient load balancing to handle the inhomogeneous dispersed phase.
Eulerian methods are simpler to implement, as they allow to simulate realistic particle concentrations, with the same numerical and parallelization approaches for both gas and liquid phase. However this comes with an increased effort in modeling issues.
This paper is devoted to the validation of the MEF as implemented in AVBP [1] in the case of Homogeneous Isotropic Turbulence (HIT). This validation is done by comparison with DPS performed with the high order NTMIX code [2].

[*]Corresponding author, aymeric.vie@ifp.fr

Equations and models for the dispersed phase

A. Mesoscopic Eulerian Formalism

Eulerian liquid conservation equations are based on the MEF developed by Février et al.[3]. Inspired by the gas kinetic theory, it defines conservation equation, starting from the Boltzmann equation [4].

The key point of this formalism is the decomposition of particle velocities v_p into a correlated part V_p common for all particles, and an uncorrelated part v'_p, proper to each particle. After statistical averaging of the particles variables over a large number of realizations, conditioned by one realization of the gas phase, equations for the liquid phase write:

$$\frac{\partial}{\partial t}\rho_l\alpha_l + \frac{\partial}{\partial x_i}\rho_l\alpha_l U_{l,i} = 0 \tag{1}$$

$$\frac{\partial}{\partial t}\rho_l\alpha_l U_{l,i} + \frac{\partial}{\partial x_j}\rho_l\alpha_l U_{l,i}U_{l,j} = \frac{\rho_l\alpha_l}{\tau_p}\left(U_{g,i}-U_{l,i}\right) - \frac{\partial}{\partial x_j}\rho_l\alpha_l\delta R_{l,ij} - \frac{\partial}{\partial x_j}\left(\frac{2}{3}\rho_l\alpha_l\delta\theta_l\delta_{ij} + P_{coll}\delta_{ij}\right) + \frac{\partial}{\partial x_i}\left(\xi_{coll}\frac{\partial}{\partial x_k}U_{l,k}\right) \tag{2}$$

$$\begin{aligned}\frac{\partial}{\partial t}\rho_l\alpha_l\delta\theta_l + \frac{\partial}{\partial x_i}\rho_l\alpha_l\delta\theta_l U_{l,i} &= -2\frac{\rho_l\alpha_l}{\tau_p}\delta\theta_l - \rho_l\alpha_l\delta R_{l,ij}\frac{\partial}{\partial x_j}U_{l,i} - \frac{\partial}{\partial x_j}\rho_l\alpha_l\delta K_{l,iij} \\ &\quad -\left(\frac{2}{3}\rho_l\alpha_l\delta\theta_l + P_{coll}\right)\frac{\partial}{\partial x_j}U_{l,j} + \rho_l\alpha_l\frac{e^2-1}{3\tau_c}\delta\theta_l + \left(\xi_{coll}\frac{\partial}{\partial x_k}U_{l,k}\right)\frac{\partial}{\partial x_i}U_{l,i}\end{aligned} \tag{3}$$

where α_l is the liquid volume fraction, U_l the correlated velocity of the MEF, and $\delta\theta_l$ the Random Uncorrelated discrete particles Energy (RUE) related to the uncorrelated velocity v'_p by the relationship $\delta\theta_l = 1/2.\langle v'_p.v'_p\rangle$. The relaxation time scale is defined as $\tau_p=\rho_l d^2/(18\mu_g)$.

B. Closure Models (with and without collisions)

The equations for the liquid phase presented previously have five unclosed terms : $\delta R_{l,ij}$, $\delta K_{l,iij}$, P_{coll} *and* ξ_{coll}. The two first terms are modeled respectively by a viscous assumption and by a diffusion term similar to Fick's law [5]:

$$\delta R_{l,iij} = -\left(\nu_{kin}+\nu_{coll}\right)\left(\frac{\partial U_{l,i}}{\partial x_j} + \frac{\partial U_{l,j}}{\partial x_i} - \frac{\partial U_{l,k}}{\partial x_k}\frac{\delta_{ij}}{3}\right) \tag{4}$$

$$\delta K_{l,iij} = -\left(\kappa_{kin}+\kappa_{coll}\right)\left(\frac{\partial\delta\theta_l}{\partial x_j}\right) \tag{5}$$

Without collision effects, P_{coll}, ξ_{coll}, ν_{coll} and κ_{coll} are zero, and ν_{kin} and κ_{kin} are written as:

$$\nu_{kin} = \frac{\tau_p}{3}\delta\theta_l, \quad \kappa_{kin} = \frac{10}{27}\tau_p\delta\theta_l \tag{6}$$

Taking into account collision changes the modeling of the kinetic viscosity and diffusion defined in Eq. 6. The principles and development of these models are reviewed in [6],[7]. The collision characteristic time scale is defined as:

$$\tau_c = \frac{d}{24 g_0\alpha_p}\sqrt{\frac{3\pi}{\delta\theta_l}}, \qquad \text{where} \qquad g_0 = \left(1-\frac{\alpha_l}{\alpha_m}\right)^{-2.5\alpha_m} \text{ and } \alpha_m = 0.64 \tag{7}$$

So that the modified kinetic viscosity and diffusivity write:

$$\nu_{kin,c} = \frac{\tau_p}{3}\delta\theta_l\left(1+\alpha_l g_0\frac{2}{5}(1+e)(3e-1)\right)\Bigg/\left(1+\frac{\tau_p}{\tau_c}\frac{(1+e)(3-e)}{10}\right) \tag{8}$$

$$\kappa_{kin,c} = \frac{2}{3}\delta\theta_l\left(1+\alpha_l g_0\frac{3}{5}(1+e)^2(2e-1)\right)\Bigg/\left(\frac{9}{5\tau_p}+\frac{(19-33e)(1+e)}{100\tau_c}\right) \tag{9}$$

where e is the elasticity coefficient. ν_{coll}, κ_{coll}, P_{coll} and ξ_{coll} are written as:

$$\nu_{coll} = \frac{4}{5}\alpha_1 g_0 (1+e)\left(\nu_{kin,c} + d\sqrt{\frac{2\delta\theta_l}{3\pi}}\right), \quad \kappa_{coll} = \alpha_1 g_0 (1+e)\left(\frac{6}{5}\kappa_{kin,c} + \frac{4}{3}d\sqrt{\frac{2\delta\theta_l}{3\pi}}\right) \tag{10}$$

$$P_{coll} = \frac{4}{3}\rho_l \alpha_l^2 g_0 (1+e)\delta\theta_l, \quad \xi_{coll} = \frac{4}{3}\rho_l \alpha_l^2 g_0 (1+e) d\sqrt{\frac{2\delta\theta_l}{3\pi}} \tag{11}$$

C. Gas phase equations

Equations for the gas phase are the classical Eulerian Navier-Stokes equations [1]:

$$\frac{\partial}{\partial t}\rho_g + \frac{\partial}{\partial x_i}\rho_g U_{g,i} = 0 \tag{12}$$

$$\frac{\partial}{\partial t}\rho_g U_{g,i} + \frac{\partial}{\partial x_j}\rho_g U_{g,i} U_{g,j} = \frac{\partial}{\partial x_j}\left(-P\delta_{ij} + \tau_{ij}\right) \tag{13}$$

$$\frac{\partial}{\partial t}\rho_g E_g + \frac{\partial}{\partial x_i}\rho_g E_g U_{g,i} = \frac{\partial}{\partial x_j}\left(-P\delta_{ij} + \tau_{ij}\right)U_{g,i} \tag{14}$$

where τ_{ij} is the stress tensor of the gas phase. This set of equation does not take into account the reduction of the gas volume fraction induced by the presence of the liquid phase. Taking into account that the dense zone correspond to a very small region of a spray, this assumption has only a weak influence.

Main characteristics of the HIT test case

The test case is a periodic cubic box sized 2π mm, meshed with 64^3 equivolumes cells. To obtain an initial turbulent gas flow field, a Passot-Pouquet spectrum is used [8]. Particles are uniformly superposed, with the same local velocity as the gas. Fig. 1a shows a gas vorticity field in the median cutting plane. A highly inhomogeneous distribution is observed. The main issue of a gas/particles HIT is that this distribution affects the particles behavior, creating preferential particle concentrations in low vorticity zones, as exhibited by Fig. 1a and Fig. 1b.

To characterize the liquid phase, the Stokes Number is introduced: $St = \tau_p/\tau_L$ where τ_L is the integral Lagrangian time scale of the gas turbulence [9]. As the same gas flow field is used for all cases (turbulence properties are listed in Table 2), the Stokes number only varies with τ_p. Three different values of τ_p were tested, for different liquid loads. Table 3 summarizes the different test cases.

Results and Discussion

All results are presented in non-dimensional variables, denoted by the superscript $^+$. The corresponding reference values are listed in Table 1.

A. Gas HIT

To check the accuracy of AVBP, using a 3rd order scheme, for HIT simulation, the decay of gaseous kinetic energy is compared to the results obtained with NTMIX, and its a 6th order scheme. The results shown in Fig. 2 are in very good agreement, confirming the validity of the AVBP simulation.

B. Gas/particule HIT

Results are analyzed in terms of preferential particle concentration and energy, compared to DPS realized by Kaufmann et al. [10]. As Elghobashi et al. shows in [11], DPS can capture essential features of particles dynamic and may be considered as a reference solution here. Simulations are run in one-way drag coupling. $< . >$ is the averaging operator over the whole domain. The preferential particle concentration is evaluated by a distribution function [12]:

$$g_{pp}^{\Delta x} = < n_p^2(\vec{x}) > / < n_p(\vec{x}) >^2 \tag{15}$$

A first test case is carried out to verify the MEF. The Stokes number is set to 1.2. Fig. 3 compares the different energy terms for both approaches (MEF and DPS) and the agreement is very good. For a better view, the uncorrelated

energy is plotted again in Fig. 4, showing a very accurate prediction of the MEF. This demonstrates the excellent behavior of the closure models for RUE terms, defined previously. Figure 5 shows the preferential particle concentration and again the good performance of MEF, compared to DPS.
Considering collisional simulations, results are analyzed qualitatively only. Figures 6 and Fig. 7 show the results for MEF simulations without collisions, then with collisions for two different loads. Preferential particle concentration and RUE both show that the model degenerates to the non-collisionnal case when the liquid volume fraction goes to 0. Furthermore, collisions increase the preferential particle concentration effect and decrease RUE. As explained by Fede et al. [13], the first effect is due to the diminution of the mean free path of the particles, acting as a the diminution of the liquid phase viscosity [14]. Concerning RUE, considering that the total energy of the particles is not affected by collisions, the effect may be only due to a modification of the energy exchange between correlated and uncorrelated motions.
To qualify the influence of the Stokes number time, the relaxation time is modified trough the liquid density. Figures 8 and Fig. 9 preferential concentration and RUE for the three cases. For lower τ_p, collisions have no effect, even with high volume fractions. When increasing τ_p, collisions effects on preferential particle concentration and RUE become more and more sensible and predominant.

Conclusions

An extension to dense sprays of the Mesoscopic Eulerian Formalism (MEF) is presented and validated. First it is shown how the MEF compares with DPS approach in the particular test case of HIT with a diluted dispersed phase.
Very good agreement is obtained in terms of energy and preferential particles concentration. In particular, the fact that total energy evolution is perfectly reproduced is very important, and demonstrates that the formalism represents the one-way drag coupling very well, without loss of energy.
This allows to add collisions and run MEF simulations to study the effects on the dispersed phase. Expected asymptotic behaviors are well exhibited, with degeneracy to non-colliding results for small liquid volume fractions.
The next step is to compare MEF results to DPS results with collisions and two-way coupling, and to investigate the importance of polydispersion (in terms of droplet diameter and velocity) in the same configuration.

Acknowledgment

Numerical computations of the Eulerian simulations were performed on the supercomputer of IFP. The authors wish to thank Dr E. Riber and Dr P. Fede for many fruitful discussions.

Nomenclature

e inelasticity coefficient
E total enthalpy
g_{pp} distribution function
n_p number of particles
U velocity
α_l liquid volume fraction
$\delta\theta_l$ random uncorrelated energy
κ diffusivity
ν viscosity
τ_c collision rate
τ_L integral time scale
τ_p relaxation time scale

Subscripts
g gas
l liquid
kin kinetic
coll collisional

Superscripts
$+$ adimensioned variable

References

1. Moureau, V., Lartigue, G., Sommerer, Y., Angelberger, C., Colin, O., and Poinsot, T., *Journal of Computational Physics* 202: 710-736 (2005).
2. Vermorel, O., Bédat,B., Simonin, O., and Poinsot, T., *Journal of Turbulence* 335: 75-109 (2003).
3. Février, P., Simonin, O., and Squires, K., *Journal of Fluid Mechanics* 533: 1-46 (2005).
4. Chapman, S., and Cowling, T., *The mathematical theory of non-uniform gazes*, Cambridge University Press, 1939.
5. Kaufmann, A. Simonin, O., and Poinsot, T., *5th International Conference on Multiphase Flow*, Yokohama, Japan, 2005.
6. Peirano, E., and Leckner, B., *Progress in Energy and Combustion Science* 24: 259-296 (1996).
7. Boelle, A., Blazer, G., and Simonin, O., *Sixth ASME Gas-Solid Flows Symposium*, Hilton Head Island, US, 1995.
8. Passot, T., and Pouquet, A., *Journal of Fluid Mechanics* 181: 441-466 (1987).
9. Hogan, R.C., Cuzzi, J.N., *Physics of Fluids* 13: 2938-2945 (2001).

10. Kaufmann, A., Moreau, M., Simonin, O., and Hélie, J., *Journal of Computational Physics* 227: 6448-6472 (2008).
11. Elghobashi, S. and Truesdell, G., *Journal of Fluid Mechanics* 242: 655-700 (1992).
12. Simonin, O., Zaichik, L.I., Alipchenkov, V.M., and Février, P., *Physics of Fluids* 18: 125107 (2006).
13. Fede, P., and Simonin, O., *Physics of Fluids* 18: 045103 (2006).
14. Martinez, L., Benkenida, A., and Cuenot, B., *21th ILASS – Europe Meeting*, Muğla, Turkey, 2007.

Table 1. References variables.

L_{ref} (m)	t_{ref} (s)	U_{ref} ($m.s^{-1}$)	μ_{ref} ($kg.m^{-1}.s^{-1}$)
10^{-3}	$2.8818\ 10^{-6}$	347.0	$2.02\ 10^{-3}$

Table 2. Gas phase properties.

$u_f'^+$	ε^+	Re_t	l_t^+	η^+	τ_L^+	τ_η^+
0.0781	0.001	12.95	0.81	0.10	4.30	2.16

Table 3. Liquid phase properties for collisional and non-collisional cases.

α_l	St	τ_p^+	ρ_l ($kg.m^{-3}$)	d_l (μm)
0.00027	1.2	5.47	1916	17.3
0.027	1.2	5.47	1916	17.3
0.027	0.6	2.73	958	17.3
0.027	2.4	10.94	3832	17.3

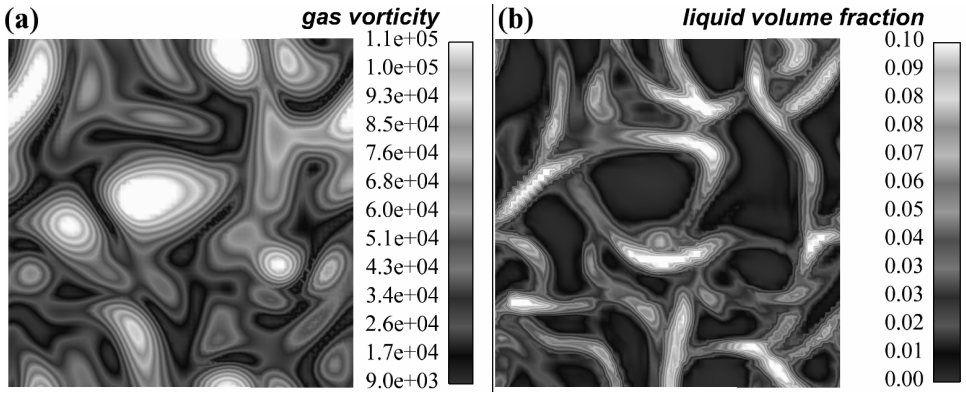

Figure 1. HIT (median cutting plane): (a) gas vorticity; (b) liquid volume fraction.

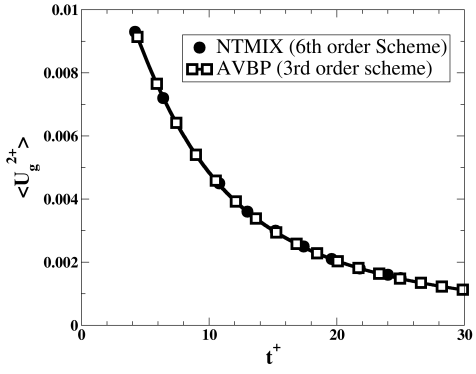

Figure 2. Gaseous kinetic energy time evolution: AVBP simulation (squares), NTMIX simulation.

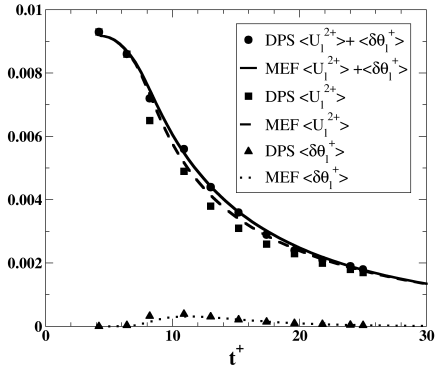

Figure 3. Liquid mean energies time evolution: total energy from DPS (circles) and MEF (solid line); correlated energy from DPS (squares) and MEF (dashed line); RUE from DPS (triangle up) and MEF (dotted line).

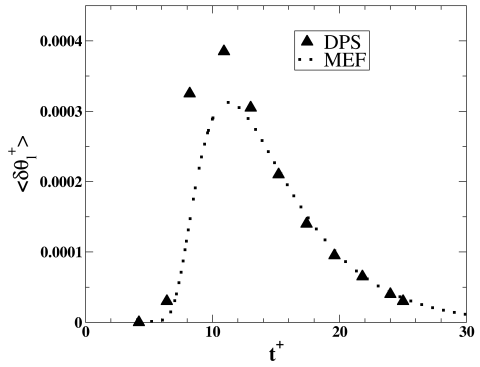

Figure 4. Mean RUE time evolution: MEF simulation (dots), DPS simulation (triangles).

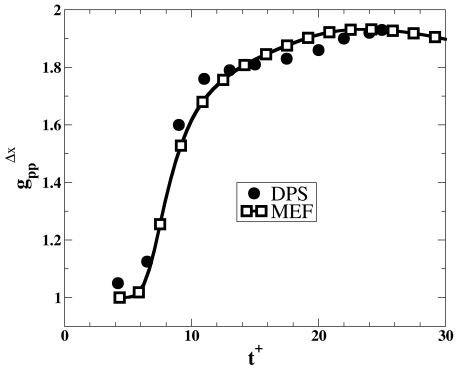

Figure 5. Preferential particle concentration time evolution: MEF simulation (squares), DPS simulation (circles).

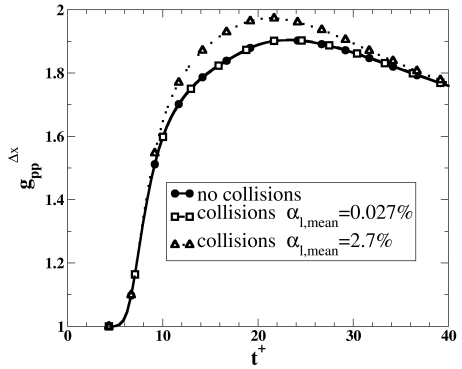

Figure 6. Preferential particle concentration time evolution of MEF simulations: without collisions (circle), with collisions at $\alpha_{l,mean}=0.027\%$ (square), with collisions at $\alpha_{l,mean}=2.7\%$ (triangle up).

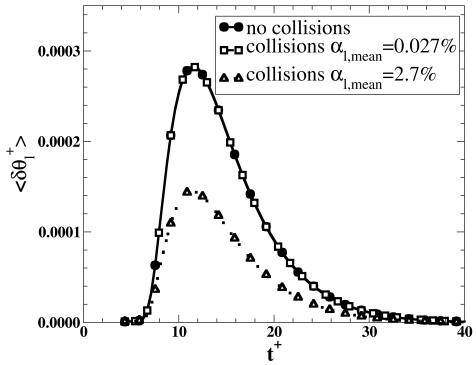

Figure 7. Mean RUE time evolution of MEF simulations: without collisions (circle), with collisions at $\alpha_{l,mean}=0.027\%$ (square), with collisions at $\alpha_{l,mean}=2.7\%$ (triangle up).

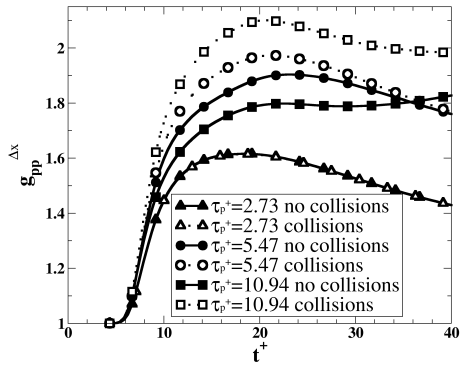

Figure 8. Preferential particle concentration time evolution of MEF simulations: with (full symbols) and without collisions (empty symbols); $\tau_p^+=2.73$ (triangles up), $\tau_p^+=5.47$ (circles) and $\tau_p^+=10.94$ (squares).

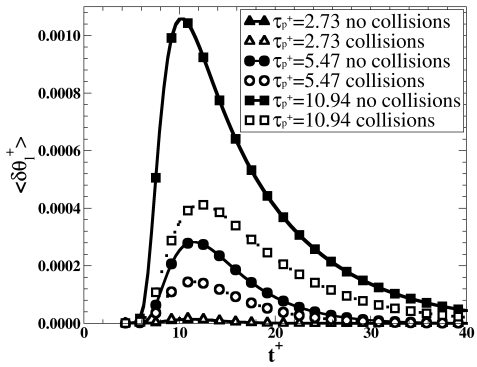

Figure 9. Mean RUE time evolution of MEF simulations: with (full symbols) and without collisions (empty symbols); $\tau_p^+=2.73$ (triangles up), $\tau_p^+=5.47$ (circles) and $\tau_p^+=10.94$ (squares).